Colloid and Interface Science Communications 50 (2022) 100668

Contents lists available at ScienceDirect

Colloid and Interface Science Communications

journal homepage: www.elsevier.com/locate/colcom

Rapid Communication

2,3-Diphospho-D-glyceric acid inhibits calciprotein particle growth and calcification in MOVAS cells but not in MC3T3-E1 cells

Davood Kharaghani *, Shohei Kohno, Tomoko Minamizaki, Tomonori Hoshino, Yuji Yoshiko *

Department of Calcified Tissue Biology, Hiroshima University Graduate School of Biomedical and Health Sciences, 1-2-3 Kasumi, Minami-Ku, Hiroshima 734-8553, Japan.

ARTICLE INFO

Keywords:
Vascular calcification
Calciprotein particles
Calcification inhibitor
2, 3-diphosphoglycerric acid
Myo-inositol hexakisphosphate

ABSTRACT

Anionic polyphosphate compounds are well-known to inhibit the formation of hydroxyapatite crystals. Vascular calcification (VC) is associated with an increase in crystalline calciprotein particles (CPPs) in the bloodstream. 2,3-Diphospho-D-glyceric acid (2,3-DPG) is a highly anionic Poly-P compound found in the concave center of erythrocytes where it binds to hemoglobin, thereby reducing oxygen affinity. Since 2.3-DPG exists in plasma, we hypothesized that 2,3-DPG may act as an endogenous inhibitor of VC. In comparison to widely recognized calcification inhibitors such as myo-inositol hexakisphosphate, 2,3-DPG significantly delayed the formation of crystalline CPPs. Additionally, 2,3-DPG inhibited calcification in a mouse vascular smooth muscle cell line (MOVAS) without cytotoxic effects. Taken together with the result that 2,3-DPG did not impact bone-like nodule formation in mouse osteoblast-like MC3T3-E1 cells, these results suggest that 2,3-DPG may inhibit VC selectively.

1. Introduction

Recent studies have indicated that calciprotein particles (CPPs) in the bloodstream are significant risk factors for vascular calcification (VC) in chronic kidney disease (CKD) and dialysis patients [1–3]. Crystalline CPPs (CPPIIs) may play a prominent role in the initiation and progression of VC [4]. Colloidal CPPs (CPPIs) are formed from a complex of proteins, including fetuin-A, albumin, and gla-rich proteins, and amorphous calcium-phosphate with an approximately 75 nm hydrodynamic radius [5]. CPPIs spontaneously transform into CPPIIs containing crystalline calcium-phosphates with an average hydrodynamic radius of 120 nm [6]. A spherical hydroxyapatite (HA) with a diameter of 100 nm to 5 μm has been observed in patients with VC [7]. *Mayer* and colleagues first demonstrated that anionic polyphosphate (Poly-P) compounds can form robust and inert chelate bonds with calcium ions present at active growth sites and dislocations on the crystal surface and prevented further deposition of calcium and phosphate [8]. Bisphosphonates (BPs) are a class of Poly-P components with the ability to inhibit VC in rats treated with warfarin, while these compounds are not recommended for the patients with advanced CKD. The reasons for this include that BPs may aggravate hyperparathyroidism and lead to adynamic bone disease, osteomalacia or mixed uremic osteodystrophy [9]. The new class of Poly-P components has therefore been introduced to reduce the side effects of BPs. *Perelló* and colleagues demonstrated that SNF472 (the hexasodium salt of myo-inositol hexaphosphate, IP6), (also known as phytic acid) can inhibit HA crystal formation at early stages or after the nucleation of calcium-phosphate by binding to the active sites of growing HA crystals [10,11]. Likewise, *Schantl* and colleagues clarified that replacing two phosphates of IP6 with two ethylene glycol oligomers to form 4,6-di-O-(methoxy-diethylene glycol)-myo-inositol-1,2,3,5-tetrakis (phosphate) improved the anti-VC effect of IP6 with reducing its chelating activity. The authors indicated that this compound could be adsorbed to the HA core of CPPs [12]. However, taken together with the result that IP6 has the potential to inhibit bone mineralization in a mouse osteoblast culture model [13], further investigation is needed to determine for the management of mineralization disorders. The concept of the mechanisms by which Poly-P compounds block HA crystal growth in VC is illustrated in Schema 1.

Grases and colleagues discovered that 2,3-Diphospho-D-glyceric acid (2,3-DPG) bound to the active cationic calcium sites of crystalline calcium oxalate monohydrate attribute to its highly negative charge and inhibit further crystal growth [14]. 2,3-DPG was discovered to regulate the allosteric properties of hemoglobin in human erythrocytes by acting as an oxygen donor [15]. 2,3-DPG is present at high concentrations not only in erythrocytes (4.5–5.0 mM) [16] but also in plasma (1.3 mM) [17]. Due to the anionic nature of 2,3-DPG, like IP6 and BPs which

* Corresponding authors.
E-mail addresses: davood@hiroshima-u.ac.jp (D. Kharaghani), yyuji@hiroshima-u.ac.jp (Y. Yoshiko).

https://doi.org/10.1016/j.colcom.2022.100668
Received 5 August 2022; Received in revised form 14 September 2022; Accepted 20 September 2022
Available online 23 September 2022

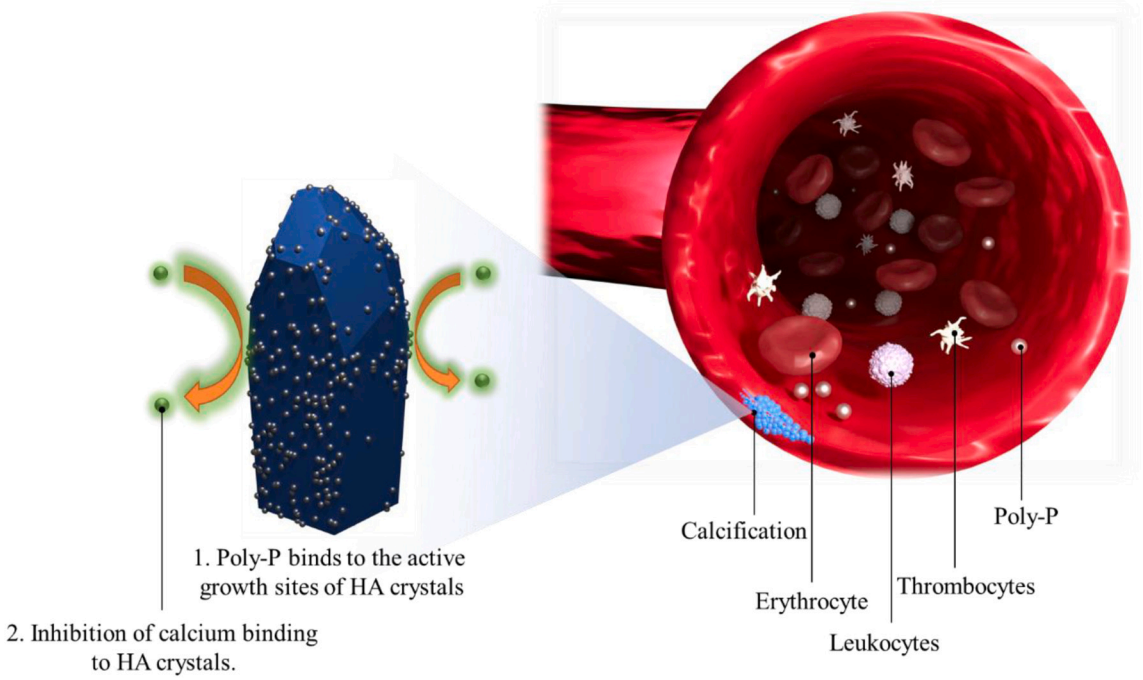

Schema 1. An illustration of a potential mechanism by which Poly-P compounds inhibit VC. Poly-P compounds with robust, inert chelate bonds to calcium ions present at active growth sites and dislocations on the HA crystal surface may prevent further calcium phosphate deposition.

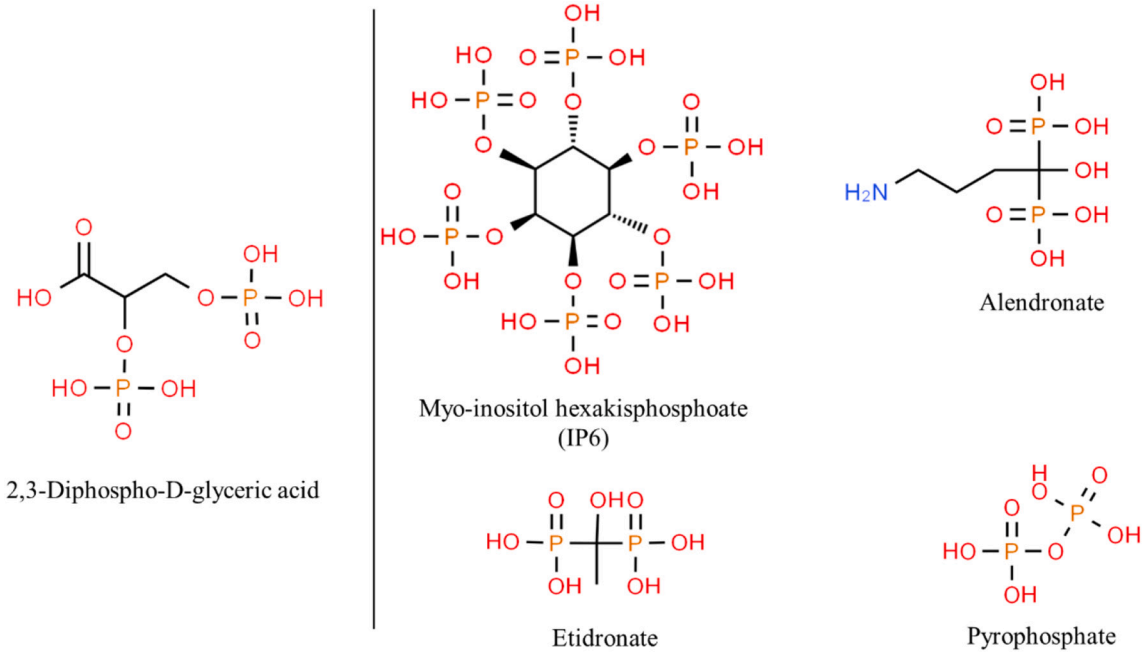

Fig. 1. The chemical structures of 2,3-DPG and well-known inhibitors of VC.

would be adsorbed onto the cationic calcium active sites of crystals [11,12,14], we hypothesize that 2,3-DPG in plasma [12] may inhibit the formation of CPPIIs and suppress VC.

Endogenous components for drug discovery offer special features in comparison to synthetic molecules. They are structurally optimized during evolution to serve particular biological functions, including the regulation of endogenous defense mechanisms. Furthermore, endogenous components used may provide insights regarding efficacy and safety [18]. Therefore, we evaluated the effect of 2,3-DPG on CPPII formation in a cell-free system and calcification in mouse vascular smooth muscle cell (MOVAS) and mouse osteoblast-like MC3T3-E1 cell cultures.

2. Methods and materials

2.1. CPP assay

CPP assay was performed as described previously [12]. Pooled human serum, (HS; BioreclamationIVT, Westbury, NY; Clinical Trials Laboratory Services, London, UK), from healthy donors (Table S1) and

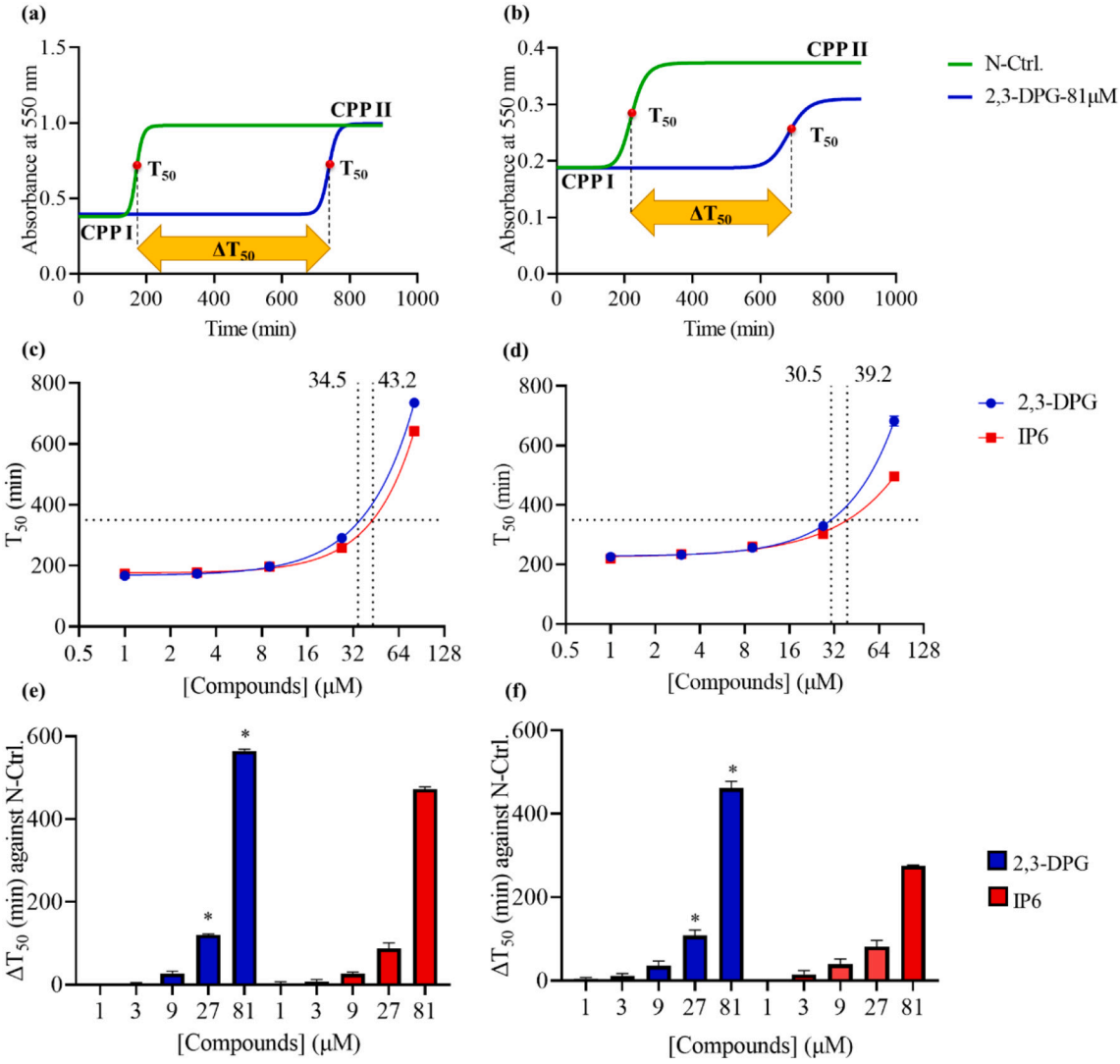

Fig. 2. The effect of 2,3-DPG and IP6 on the transformation of CPPIs to CPPIIs. Representative data for CPPII formation in the presence of HS (a) and FBS (b) with and without 81 μM 2,3-DPG. The concentration necessary to delay T_{50} to 350 min in the presence of HS (c) and FBS (d) with and without 2,3-DPG and IP6 and corresponding ΔT_{50} (min) in HS (e) and FBS (f). (mean ± SD, * $p < 0.0001$ vs. IP6 at same concentrations). n = 5.

fetal bovine serum, (FBS; F7524, Sigma, Burlington, MA, United States), were stored at −80 °C until use. HS and FBS were thawed at room temperature (RT) and centrifuged at 10,000*g*, 4 °C for 30 min. The supernatants were then filtered (25CS020AS, Advantec, Ehime, Japan) to remove cryoprecipitates. Calcium chloride (036–19,731, Wako Chemical, Miyazaki, Japan) solution with a concentration of 40 mM in HEPES (346–01373, FUJIFILM Wako Chemical, Osaka, Japan)/NaCl (191–01665, Wako Chemical) buffered saline (HBS) (100 mM HEPES, 140 mM NaCl) solution, was prepared, pH 7.4 at RT. A phosphate solution containing 19.44 mM Na_2HPO_4 (106,580, Merck, Darmstadt, Germany) and 4.56 mM NaH_2PO_4 (28–3790-5, Sigma) with the final concentration of 24 mM PO_4 was prepared using HBS, pH 7.4 at RT. All salt solutions were double sterilized filtered, and pre-warmed at 37 °C prior to use. Calcium solution, HS or FBS, phosphate solution, 2,3-Diphospho-D-glyceric acid pentasodium salt (2,3-DPG), (D5764, Sigma) in Milli-Q water or phytic acid sodium salt hydrate (IP6), (P8810-10G, Sigma), solutions in Milli-Q water were mixed at a volume ratio of 5:8:5:2 in microtubes respectively and transferred to a non-coated 96-well plate (167,008, Thermo Scientific, Massachusetts, United States) with a final volume of 200 μL. Final concentrations of 2,3-DPG or IP6 were 1, 3, 9, 27, and 81 μM. For the negative control (N-Ctrl.), Milli-Q water was used as a substitute for 2,3-DPG and IP6 solutions. The plate was sealed with a transparent adhesive film (Watson, 547-KTS-HCP, Japan), and absorbance at 550 nm was measured every 3 min at 37 °C with background shaking for 30 s and waiting for 1 min in a shaker microplate reader (Varioskan Flash, Thermo Fisher Scientific). Time-dependent absorbance graph, and T_{50} against the concentrations (μM) graph, calculating nonlinear regression was drown using GraphPad Prism 9 and Eq. (1) whereby X = [2,3-DPG], Y = time (min), bottom = baseline response, top = maximum response, T_{50} = [2,3-DPG or IP6] that lead to half-maximum response, and hillslope = steepness of the curve. The activity of 2,3-DPG and IP6 against N-Ctrl. to delay CPPII formation was compared, generating ΔT_{50} (min) against concentration (μM).

$$Y = Bottom + \frac{(Top - Bottom)}{1 + \left(\frac{T50}{X}\right)^{Hill\ Slope}} \quad (1)$$

2.2. Cell proliferation, cytotoxicity, and morphology

We assessed the effect of 2,3-DPG, on cell proliferation in mouse osteoblast-like MC3T3-E1 and vascular smooth muscle MOVAS cells using Thiazolyl Blue Tetrazolium Bromide (MTT) (M5655, Sigma). For quantitative measurement of lactate dehydrogenase (LDH) release level,

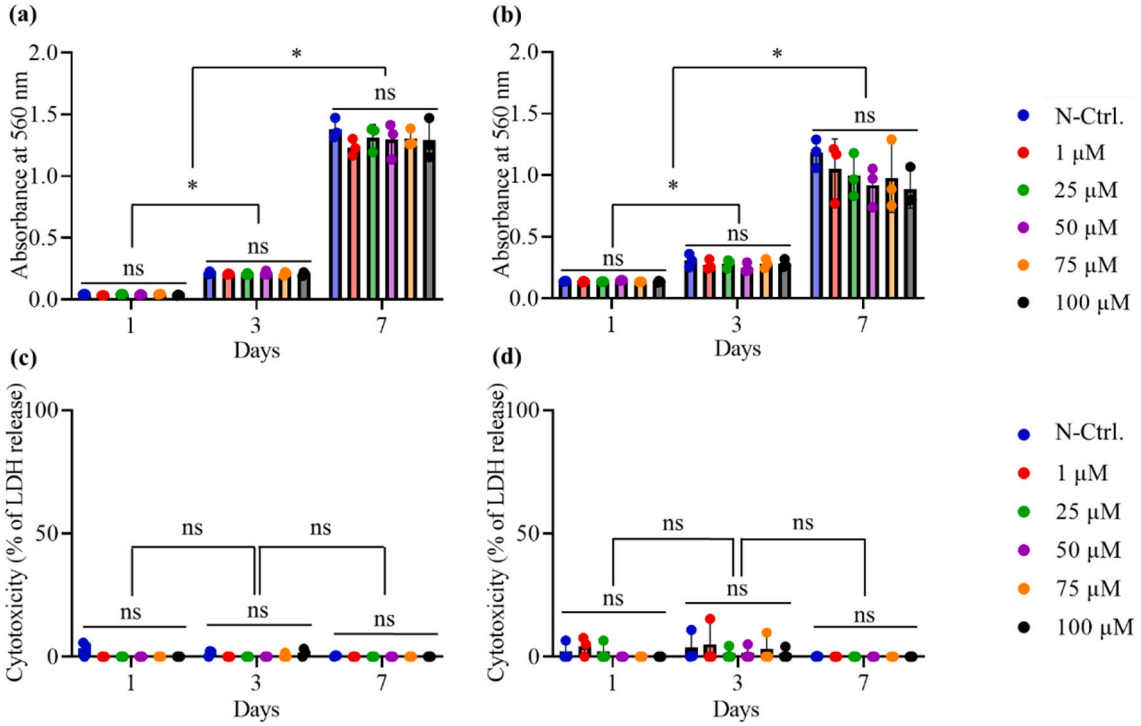

Fig. 3. The effects of 2,3-DPG on cell proliferation and cytotoxicity. MC3T3-E1 cells (a and c) and MOVAS cells (b and d) were treated with or without 2,3-DPG for 1, 3, and 7 days. (Data are shown as mean ± SD, ns: $p > 0.05$ no significant difference, * $p < 0.0001$ for other comparisons). $n = 3$.

the Cytotoxicity LDH assay kit-WST (Dojindo molecular technologies, Kumamoto, Japan) was also used according to the manufacturer's instruction. Cells at 1000 cells/cm^2 in a 96-well plate were cultured in αMEM (MC3T3-E1; 135–15,175, Wako Chemical) or D-MEM high glucose (MOVAS; 043–30,085, Wako Chemical), supplemented with 10% (*v*/v) FBS, 100 units/mL penicillin (P3032-25MU, Sigma), and 100 μg/mL streptomycin (S9137-25G, Sigma) at 37 °C with 5% CO_2. The next day, cells were exposed to a fresh medium with or without 2,3-DPG at different concentrations for the indicated time points. Medium was changed every second or third day, unless otherwise specified. In order to determine cell proliferation at each time point, 10 μL of 0.5 mg/mL MTT solution in PBS was added to each well and followed by incubation for 4 h in a humidified incubator at 37 °C with 5% CO_2. Medium was then removed, and formazan crystals were dissolved in dimethyl sulfoxide (DMSO) (043–07216, Wako Chemical) (100 μL). The cytotoxicity of different concentrations of 2,3-DPG was ensured by cultivating MC3T3-E1, and MOVAS cells in the same manner previously explained for cell proliferation. The absorbance was measured at 560 nm (MTT) and 490 nm (LDH) using a microplate reader (Promega™ GloMax® Explorer Micro Plate Reader, Wisconsin, United States). Cytotoxicity percentage was expressed as Eq. (2). A, B and C represents the test substances, highly toxic (lysis buffer) positive control, and non-treated cells as low toxic control (N-Ctrl.) respectively.

$$Cytotoxicity\ (\%) = \frac{(A - C)}{(B - C)} \times 100 \quad (2)$$

To evaluate the effect of 2,3-DPG or IP6 at different concentrations on cell morphology, cells were cultured for 72 h with as described above. Cells were then washed three times with PBS, fixed with 4% paraformaldehyde in PBS (PFA) (163–20,145, Wako Chemical) for 20 min, and permeabilized with 0.5% Triton X-100 (30–5140, Katayama Chemical, Osaka, Japan) in PBS. Cells were then stained with ActinGreen™ 488 ReadyProbes™ reagent (AlexaFluor 488 phalloidin, R37110, Invitrogen, Massachusetts, United States), based on the manufacturer's protocol. Cells were counterstained with DAPI (D523, Dojindo molecular technologies) diluted (1:2000) in 20 mM Tris-HCL (T1378, Sigma), containing 150 mM NaCl, pH 7.4, and examined under a microscope (All-in-One Fluorescence Microscope BZ-X810, Keyence, Osaka, Japan).

2.3. CPPII preparation

CPPII solution was prepared as described previously [12] with slight modifications. Briefly, double sterilized filtered 140 mM NaCl solution, cleared FBS, 24 mM phosphate solution, and 40 mM calcium solution were combined at a volume ratio of 2:8:5:5, and mixed on gentle agitation (150 rpm) at 37 °C for 17 h in a 50 mL falcon tube, followed by centrifugation at 20,000*g*, 4 °C for 2.5 h. The pellets were then washed twice with ice-cold HBS and resuspended in 50 μL of HBS at 37 °C. The resultant colloidal solutions were pooled and centrifuged at 1000*g* for 10 min at RT. Aliquots of supernatants (CPPII solution) were snap-frozen in liquid nitrogen and stored at −80 °C until use for no longer than two months. 50 μL of CPPII solution was diluted with 450 μL of 0.6 M HCl (080–01066, Wako Chemical), and the quantitative amount of calcium was measured using calcium colorimetric kit (437–58,201, Calcium *E*-test, Wako Chemical).

2.4. Calcification in MOVAS cell cultures

MOVAS cells were seeded at 10,000 cells/cm^2 in a 48-well plate and cultured as described above. After 24 h, cells were exposed to fresh medium including CPPIIs (20 μg Ca/mL) and 1 mM Ca^{2+} (calcium chloride) for additional 7 days to induce calcification. Calcification could be detected, when cells were treated with a combination of CPPIIs and Ca^{2+}, but neither with Ca^{2+} alone nor with CPPIIs alone. Cells were fixed with 4% PFA for 20 min, washed with PBS and stained with Alizarine Red S (2% *w/v*) for 5 min. To quantify calcium levels, cells were washed twice with PBS and decalcified overnight at 4 °C with 100 μL/well of 0.6 M HCl. The supernatants were then collected, and calcium content was determined using a calcium colorimetric kit. Subsequently, cells were washed with PBS and lysed in 0.1 M NaOH and 0.1% w/v sodium dodecyl sulfate (100 μL) for 2 h. Protein content was quantified

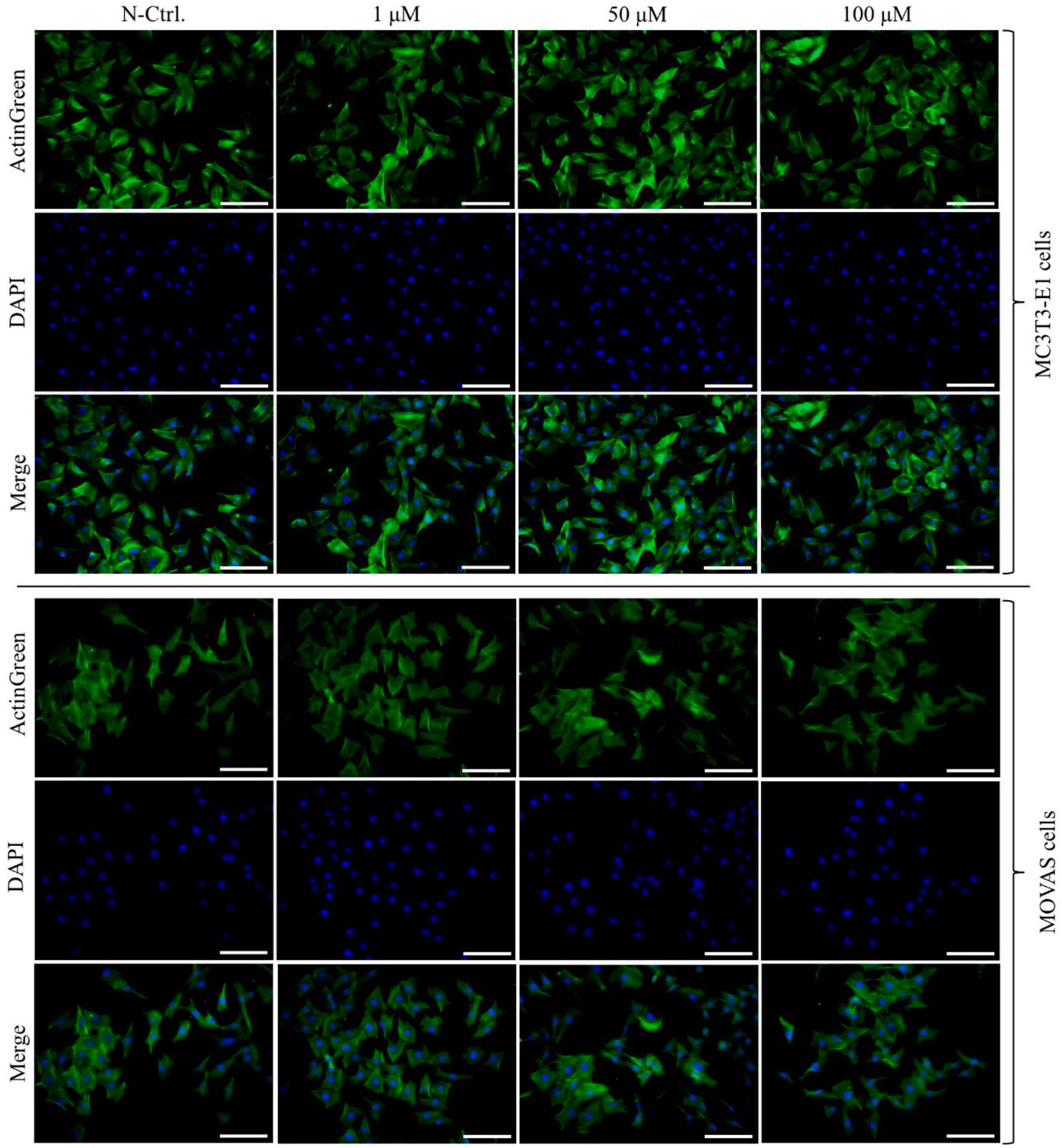

Fig. 4. The effect of 2,3-DPG on the morphology of MC3T3-E1 cells and MOVAS cells. Cells were treated with or without 2,3-DPG for 72 h. Cytoskeleton, ActinGreen™ 488 ReadyProbes™ (green); Nucleus DAPI (blue). Scale bar, 200 μm. (For interpretation of the references to colour in this figure legend, the reader is referred to the web version of this article.)

using a Pierce BCA Protein Assay Kit (23,227, Thermo Scientific) and the calcium equivalent to the protein.

2.5. Calcification in MC3T3-E1 cell cultures

MC3T3-E1 cells were seeded at 3000 cells/cm^2 in a 48-well plate and cultured as described above. The next day, cells were exposed to fresh medium additionally supplemented with 50 μg/mL L-ascorbic acid (AA), (321–44,823, Wako Chemical) and 10 mM of β-glycerol phosphate (βGP), (G9891, Sigma), (osteogenic medium) [19] in the presence or absence of 2,3-DPG and IP6 with medium changing every 2 or 3 days. At day 10, cells were washed with PBS and fixed with 4% PFA for 20 min. To demonstrate bone-like nodules, cells were subjected to alkaline phosphatase and von Kossa staining. Briefly, washed cells were treated

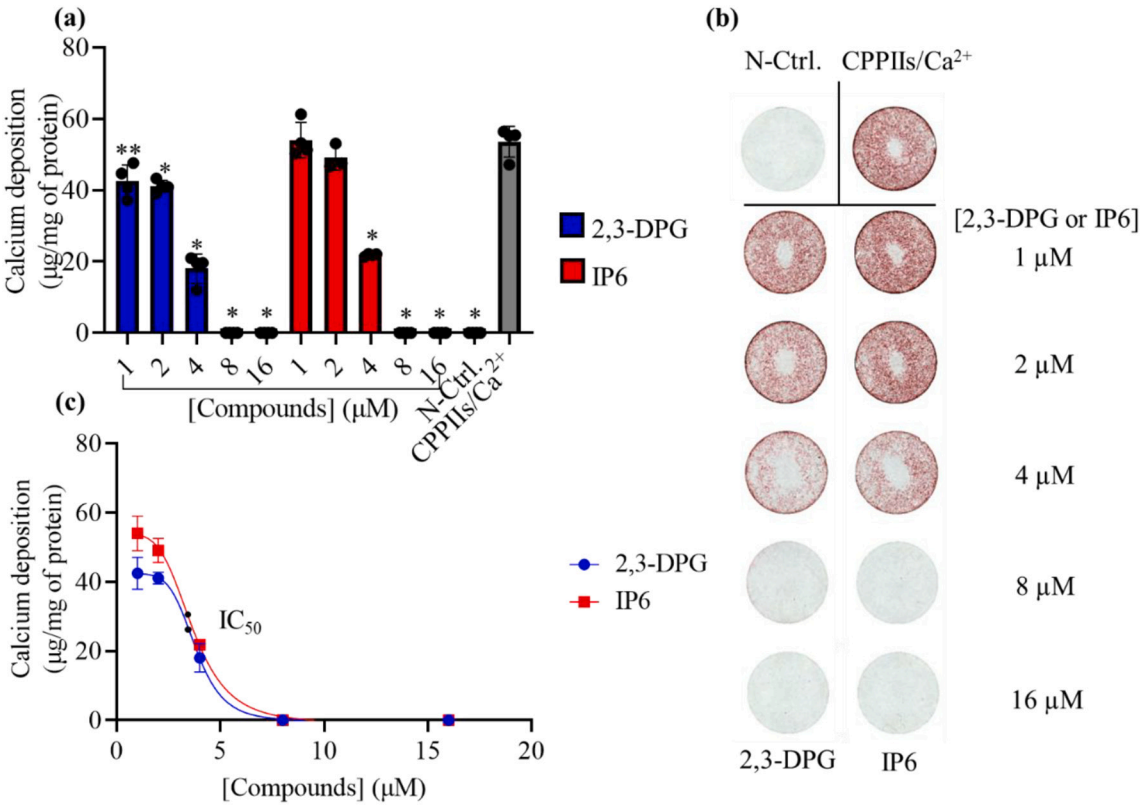

Fig. 5. The effect of 2,3-DPG and IP6 on calcification in MOVAS cell cultures. Cells were treated with or without 2,3-DPG and IP6 for 7 days in the presence of CPPIIs and Ca^{2+} (CPPIIs/ Ca^{2+}). Calcium deposition (a), and representative images of Alizarin Red S staining (b) are shown. IC_{50} values for 2,3-DPG and IP6 were also exhibited (c). (Data are shown as mean ± SD, * $p < 0.0001$ and ** $p < 0.0003$ compared with CPPIIs/ Ca^{2+}). $n = 4$. (For interpretation of the references to colour in this figure legend, the reader is referred to the web version of this article.)

with 200 μL of 0.5 mg/mL Red violet LB salt (F3381-1G, Sigma) in 0.1 M Tris-HCl solution (pH 8.3) containing 1 mg/mL Naphthol As-MX phosphate (N4575-1G), and 4 μL/mL *N,N*-Dimethylformamide (13016–94, Nacalai Tesque, Kyoto, Japan). The plate was incubated at RT for 1 h and washed well with Milli-Q water. Von Kossa staining was performed by incubating the plate with a 2.5% silver nitrate (28–1310-5, Sigma-Aldrich) solution for 45 min and washing with Milli-Q water 3 times (5 min for each wash). ImageJ was used to measure areas of ALP/von Kossa-positive bone-like nodules.

2.6. Statistical analysis

Statistical significance was calculated from a one-way ANOVA, followed by Tukey's multiple comparison test using GraphPad Prism 9.

3. Results and discussion

3.1. CPP assay

A comparison of the chemical structures of 2,3-DPG with known Poly-P compounds demonstrating the inhibitory activity in VC, as shown in Fig. 1. Considering the ability of 2,3-DPG in binding to calcium active sites of calcium oxalate crystals [15], we hypothesized that 2,3-DPG may inhibit CPPII formation via a possible mechanism by which highly anionic phosphates of this compound may bind to calcium active sites of HA crystals.

As described elsewhere [20], the transformation of CPPIs to crystalline CPPIIs in a cell-free system was detected along with an increase in absorbance at a visual wavelength (550 nm). To compare the effect of 2,3-DPG with that of IP6 time-resolved spectroscopy was employed to monitor the 50% phase transition (T_{50}) of CPPIs to CPPIIs as shown in Fig. 2 (a and b). The results indicated that 2,3-DPG suppressed the transformation of CPPIs to CPPIIs in a dose-dependent manner. Fig. S1 indicated the entire data related to a delay in transformation of CPPIs to CPPIIs in HS and FBS. To compare the dose-dependent inhibitory activity of 2,3-DPG and IP6, T_{50} and ΔT_{50} (T_{50} against the N-Ctrl.) vs. concentration graphs were generated. 2,3-DPG significantly delayed the transformation of CPPIs to CPPIIs at concentrations of >27 μM in both HS and FBS, as shown in Fig. 2c-f. Besides, T_{50} demonstrated that 2,3-DPG appeared slightly stronger than IP6, even though the former was 43% lower molecular weight (calculated based on Eq. (3)) and a smaller number of phosphates than IP6. Molecular weight is an essential consideration for dosing purposes and hyperphosphatemia [12].

$$Mw\% = \frac{\mathrm{Mw}_{\mathrm{IP6}} - Mw_{2,3-DPG}}{Mw_{IP6}} \times 100 \quad (3)$$

Moreover, doses of 2,3-DPG and IP6 to delay the transformation of CPPIs to CPPIIs at 350 min was compared [12]. Concentrations necessary to delay T_{50} to 350 min in HS was calculated at 34.5 and 43.2 μM for 2,3-DPG and IP6, respectively. Similar results were obtained, when FBS was used as a source of CPP (30.5 μM for 2,3-DPG and 39.2 μM for IP6), as shown in Table S1 and Fig. 2 (c and b). Difference in concentrations at T_{50} between HS and FBS may be due to biochemical and biophysical features of human and bovine Fetuin-A and other CPP components proteins such as albumin [21] that need further investigation.

3.2. Cell proliferation and LDH release

In human erythrocytes, 2,3-DPG is the most abundant phosphate containing compound (5 mM) even more than ATP (1.3 mM) [22]. Since this concentration may be intracellular especially in erythrocytes, we examined the effect of 2,3-DPG on cell proliferation and toxicity in

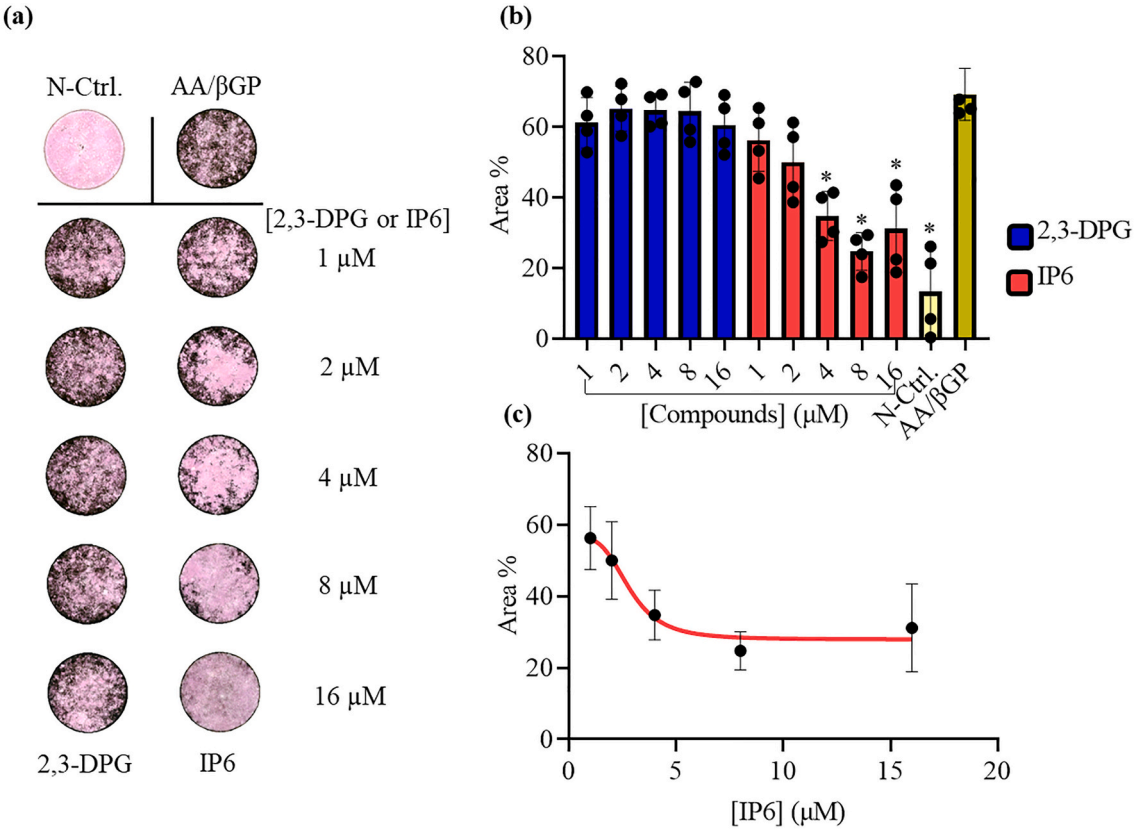

Fig. 6. The effects of 2,3-DPG and IP6 on calcification in MC3T3-E1 cell culture. Cells were treated with or without 2,3-DPG and IP6 for 10 days in presence of AA and βGP. Representative images of ALP and Von Kossa staining, indicating bone-like nodule formation (a), ImageJ was used to measure area (%) of calcification (b), and the IC_{50} for IP6 was determined. (Data are shown as mean ± SD, * $p < 0.0001$, compared with treated cells via AA and βGP in absence of 2,3-DPG or IP6). $n = 4$.

MC3T3-E1 and MOVAS cells. Cells were treated with 2,3-DPG at different concentrations include >27 μM that could inhibit the transformation of CPPIs to CPPIIs. MTT assay indicated that 2,3-DPG had no adverse effect on the proliferation even at higher concentrations necessary to delay T_{50} to 350 min in HS or FBS, (Fig. 3a, b). Release of LDH from cells treated with 2,3-DPG even at 100 μM were <5% compared with positive control (treated cells with lysis buffer), indicating a minimum level of cytotoxicity as shown in Fig. 2.

We also evaluated morphology, one of the essential aspects of cell phenotypes that regulates cell activities [23]. The effect of 2,3-DPG and IP6 on MC3T3-E1 and MOVAS cells was evaluated after 72 h. Staining with ActinGreen™ 488 ReadyProbes™ Reagent and DAPI showed that morphology of MC3T3-E1 cells and MOVAS cells were treated with 2,3-DPG, was similar to the negative control (N-Ctrl.; non-treated cells), as shown in Fig. 4 (for 2,3-DPG) and Fig. S2 (for IP6). The results indicated signs of cell-cell interaction with a flattened morphology, suggesting an excellent adhesion to the bottom multiwell plates. The results demonstrated that even a high dosage of 2,3-DPG or IP6 (100 μM; more than the required dosage to delay T_{50} to 350 min) did not have any adverse effect on MC3T3-E1 and MOVAS cell.

3.3. Calcification in MOVAS cell cultures

The effect of 2,3-DPG and IP6 on calcification in MOVAS cell cultures was examined in the presence or absence of 20 μg Ca/mL CPPIIs and 1 mM/mL Ca^{2+} for 7 days. Calcification could be detected only in a combination of CPPIIs and Ca^{2+} (CPPIIs/ Ca^{2+}) but not CPPIIs alone or Ca^{2+} alone, as shown in Fig. 5 and Fig. S3. As a further evaluation of the effect of CPPII and Ca^{2+} accumulation without cellular activity, fixed MOVAS cells with 4% PFA, did not show any CPPIIs/ Ca^{2+} dependent calcification (Fig. S4), suggesting that the activity of MOVAS cells implicated in calcification process. The results from Alizarine Red S staining indicated that 2,3-DPG and IP6 inhibited calcification at concentrations >8 μM. From the quantitative measurement of calcium deposition, IC_{50} was calculated 3.8 and 3.7 μM for 2,3-DPG and IP6 respectively. The results showed that 2,3-DPG inhibited calcification perfectly at the concentrations >4 μM. (See Fig. 6.)

3.4. Calcification in MC3T3-E1 cell

MC3T3-E1 cells were cultured in the osteogenic medium containing 50 μg/mL of the AA, and 10 mM of βGP with or without 2,3-DPG and IP6 at same concentrations that MOVAS cells was treated. Medium supplemented with AA and βGP was used for 2,3-DPG and IP6 treated cells and medium without βGP was chosen as negative control (N-Ctrl.). The inhibitory effect of IP6 was seen at concentrations >2 μM (IC_{50} = 2.8 μM) in agreement with *Addison* and colleagues, that demonstrated a dose-dependent inhibition of mineralization in MC3T3-E1 cell cultures [24]. However, 2,3-DPG even at a concentration of 16 μM had no significant impact on calcification in MC3T3-E1 cell cultures as shown in Fig. 5. This may be caused due to 2,3-DPG involvement in osteoblast glycolysis. *Liu* and colleagues showed that treatment of mouse osteoblast-like RD-C6 cells via rhBMP2 upregulated multiple genes including 2,3-bisphosphoglycerate mutase (Bpgm) [25], which is closely related to the glycolytic housekeeping enzyme MPGM. BPGM and MPGM are structurally homologous and provide a rationale for the specific residues that are crucial for synthase, mutase, and phosphatase activity [26]. These results suggest that 2,3-DPG might be easily degraded in osteoblasts. However, further investigation is needed to determine the mechanisms underlying selective inhibitory activity of 2,3-DPG in calcification.

4. Conclusion

Our study demonstrated for the first time that 2,3-DPG can inhibit calcification in mouse vascular smooth muscle MOVAS cells selectively. Compared with IP6, 2,3-DPG significantly attenuated the progression of CPPI transformation to CPPII. In contrast, 2,3-DPG did not affect calcification in MC3T3-E1 cell cultures. 2,3-DPG also showed excellent safety in biological environments regarding cell proliferation, cytotoxicity tests and cell morphology. This finding suggests that calcification is selectively inhibited in MOVAS cells but not in MC3T3-E1 cells. Current research demands further evaluations to demonstrate in vivo effects of 2,3-DPG for therapeutic applications in VC and ectopic calcification. The mechanisms that underlie 2,3-DPG metabolism in osteoblasts, as well as the effect of 2,3-DPG on HA crystal formation, should also be investigated.

Funding

This work was supported by JSPS KAKENHI Grant-in-Aid for Scientific Research (C) 21K09816.

CRediT authorship contribution statement

Davood Kharaghani: Conceptualization, Software, Validation, Resources, Data curation, Writing – original draft, Writing – review & editing, Visualization, Supervision, Project administration. **Shohei Kohno:** Data curation, Writing – review & editing. **Tomoko Minamizaki:** Data curation, Writing – review & editing. **Tomonori Hoshino:** Data curation, Writing – review & editing. **Yuji Yoshiko:** Validation, Resources, Data curation, Writing – review & editing, Visualization, Supervision.

Declaration of Competing Interest

The authors declare no conflict of interest.

Data availability

Data will be made available on request.

Appendix A. Supplementary data

Supplementary data to this article can be found online at https://doi.org/10.1016/j.colcom.2022.100668.

References

[1] E.R. Smith, F.F.M. Pan, T.D. Hewitson, N.D. Toussaint, S.G. Holt, Effect of sevelamer on calciprotein particles in hemodialysis patients: the sevelamer versus calcium to reduce Fetuin-A-containing calciprotein particles in dialysis (SCaRF) randomized controlled trial, Kidney Int. Rep. 5 (2020) 1432–1447.
[2] C.N. Silaghi, T. Ilyés, A.J. van Ballegooijen, A.M. Crăciun, Calciprotein particles and serum calcification propensity: hallmarks of vascular calcifications in patients with chronic kidney disease, J. Clin. Med. 9 (2020) 1287.
[3] M.M.X. Cai, E.R. Smith, S.-J. Tan, T.D. Hewitson, S.G. Holt, The role of secondary Calciprotein particles in the mineralisation paradox of chronic kidney disease, Calcif. Tissue Int. 101 (2017) 570–580.
[4] C.N. Silaghi, T. Ilyés, A.J. van Ballegooijen, A.M. Crăciun, Calciprotein particles and serum calcification propensity: hallmarks of vascular calcifications in patients with chronic kidney disease, J. Clin. Med. 9 (2020) 1287.
[5] M. Bäck, T. Aranyi, M.L. Cancela, M. Carracedo, N. Conceição, G. Leftheriotis, V. Macrae, L. Martin, Y. Nitschke, A. Pasch, Endogenous calcification inhibitors in the prevention of vascular calcification: a consensus statement from the COST action EuroSoftCalcNet, Front. Cardiovasc. Med. 5 (2019) 196.
[6] Y. Miura, Y. Iwazu, K. Shiizaki, T. Akimoto, K. Kotani, M. Kurabayashi, H. Kurosu, M. Kuro-o, Identification and quantification of plasma calciprotein particles with distinct physical properties in patients with chronic kidney disease, Sci. Rep. 8 (2018) 1–16.
[7] S. Bertazzo, E. Gentleman, K.L. Cloyd, A.H. Chester, M.H. Yacoub, M.M. Stevens, Nano-analytical electron microscopy reveals fundamental insights into human cardiovascular tissue calcification, Nat. Mater. 12 (2013) 576–583.
[8] J.L. Meyer, G.H. Nancollas, The influence of multidentate organic phosphonates on the crystal growth of hydroxyapatite, Calcif. Tissue Res. 13 (1973) 295–303.
[9] U.A.A.S. el Din, M.M. Salem, D.O. Abdulazim, Vascular calcification: when should we interfere in chronic kidney disease patients and how? World J. Nephrol. 5 (2016) 398.
[10] M.D. Ferrer, M. Ketteler, F. Tur, E. Tur, B. Isern, C. Salcedo, P.H. Joubert, G. J. Behets, E. Neven, P.C. D'Haese, Characterization of SNF472 pharmacokinetics and efficacy in uremic and non-uremic rats models of cardiovascular calcification, PLoS One 13 (2018), e0197061.
[11] J. Perelló, M.D. Ferrer, M. del Mar Pérez, N. Kaesler, V.M. Brandenburg, G. J. Behets, P.C. D'Haese, R. Garg, B. Isern, A. Gold, Mechanism of action of SNF472, a novel calcification inhibitor to treat vascular calcification and calciphylaxis, Br. J. Pharmacol. 177 (2020) 4400–4415.
[12] A.E. Schantl, A. Verhulst, E. Neven, G.J. Behets, P.C. D'Haese, M. Maillard, D. Mordasini, O. Phan, M. Burnier, D. Spaggiari, Inhibition of vascular calcification by inositol phosphates derivatized with ethylene glycol oligomers, Nat. Commun. 11 (2020) 1–17.
[13] W.N. Addison, M.D. McKee, Inositol hexakisphosphate inhibits mineralization of MC3T3-E1 osteoblast cultures, Bone. 46 (2010) 1100–1107.
[14] F. Grases, C. Genestar, J. Palou, Study of the effects of several related phosphorus derivatives of biological interest in calcium oxalate crystal growth, Colloids Surf. A Physicochem. Eng. Asp. 44 (1990) 29–34.
[15] R. Benesch, R.E. Benesch, The effect of organic phosphates from the human erythrocyte on the allosteric properties of hemoglobin, Biochem. Biophys. Res. Commun. 26 (1967) 162–167.
[16] E. Tellone, D. Barreca, A. Russo, A. Galtieri, S. Ficarra, New role for an old molecule: the 2, 3-diphosphoglycerate case, Biochim. Biophys. Acta (BBA) Gen. Subj. 1863 (2019) 1602–1607.
[17] I. Stangerup, N.L. Kramp, A.K. Ziegler, F. Dela, K. Magnussen, J.W. Helge, Temporary impact of blood donation on physical performance and hematologic variables in women, Transfusion (Paris) 57 (2017) 1905–1911.
[18] A.L. Harvey, Natural products in drug discovery, Drug Discov. Today 13 (2008) 894–901.
[19] T. Minamizaki, Y. Nakao, Y. Irie, F. Ahmed, S. Itoh, N. Sarmin, H. Yoshioka, A. Nobukiyo, C. Fujimoto, S. Niida, The matrix vesicle cargo miR-125b accumulates in the bone matrix, inhibiting bone resorption in mice, Commun. Biol. 3 (2020) 1–11.
[20] A. Pasch, S. Farese, S. Gräber, J. Wald, W. Richtering, J. Floege, W. Jahnen-Dechent, Nanoparticle-based test measures overall propensity for calcification in serum, J. Am. Soc. Nephrol. 23 (2012) 1744–1752.
[21] Y.-H. Lin, V. Franc, A.J.R. Heck, Similar albeit not the same: in-depth analysis of proteoforms of human serum, bovine serum, and recombinant human fetuin, J. Proteome Res. 17 (2018) 2861–2869.
[22] N.V. Bhagavan, Chapter 28 - Hemoglobin, in: N.V. Bhagavan (Ed.), Medical Biochemistry, Fourth edition, Academic Press, San Diego, 2002, pp. 645–674.
[23] C.K. Kuo, W.-J. Li, R.S. Tuan, Chapter II.6.8 - Cartilage and ligament tissue engineering: biomaterials, cellular interactions, and regenerative strategies, in: B. D. Ratner, A.S. Hoffman, F.J. Schoen, J.E. Lemons (Eds.), Biomaterials Science, Third edition, Academic Press, 2013, pp. 1214–1236.
[24] W.N. Addison, M.D. McKee, Inositol hexakisphosphate inhibits mineralization of MC3T3-E1 osteoblast cultures, Bone. 46 (2010) 1100–1107.
[25] T. Liu, Y. Gao, K. Sakamoto, T. Minamizato, K. Furukawa, T. Tsukazaki, Y. Shibata, K. Bessho, T. Komori, A. Yamaguchi, BMP-2 promotes differentiation of osteoblasts and chondroblasts in Runx2-deficient cell lines, J. Cell. Physiol. 211 (2007) 728–735.
[26] R. van Wijk, W.W. van Solinge, The energy-less red blood cell is lost: erythrocyte enzyme abnormalities of glycolysis, Blood. 106 (2005) 4034–4042.